NMR investigation of vortex dynamics in the $Ba(Fe_{0.93}Rh_{0.07})_2As_2$ superconductor

L. Bossoni,[1,2] P. Carretta,[1] A. Thaler,[3] and P. C. Canfield[3]
[1]*Department of Physics, "A. Volta" University of Pavia-CNISM, I-27100 Pavia, Italy*
[2]*Department of Physics, "E. Amaldi" University of Roma Tre-CNISM, I-00146 Roma, Italy*
[3]*Ames Laboratory, US DOE, and Department of Physics and Astronomy, Iowa State University, Ames, Iowa 50011, USA*
(Received 19 December 2011; revised manuscript received 15 March 2012; published 28 March 2012)

^{75}As NMR spin-lattice relaxation ($1/T_1$) and spin-echo decay ($1/T_2$) rate measurements were performed in a single crystal of $Ba(Fe_{0.93}Rh_{0.07})_2As_2$ superconductor. Below the superconducting transition temperature T_c, when the magnetic field **H** is applied along the c axes, a peak in both relaxation rates is observed. Remarkably that peak is suppressed for $\mathbf{H} \perp c$. Those maxima in $1/T_1$ and $1/T_2$ have been ascribed to the flux lines lattice motions and the corresponding correlation times and pinning energy barriers have been derived on the basis of a heuristic model. Further information on the flux lines motion was derived from the narrowing of ^{75}As NMR linewidth below T_c and found to be consistent with that obtained from $1/T_2$ measurements. All the experimental results are described in the framework of thermally activated vortices motions.

DOI: 10.1103/PhysRevB.85.104525 PACS number(s): 74.25.nj, 74.25.Wx, 74.25.Uv

I. INTRODUCTION

The recent discovery of iron-based superconductors[1] was welcomed by the scientific community, because it was supposed to answer the still open questions regarding the pairing mechanism in high-temperature superconductors. However, the multiplicity of controversial experimental results suggests that a unique description of the superconducting properties is far from being reached. Among the still debated fundamental topics, e.g., the order-parameter symmetry,[2–6] the nanoscopic coexistence of magnetism with superconductivity,[7,8] the role of antiferromagnetic spin fluctuations in the pairing mechanism,[9–11] one fixed point is represented by the study of the flux lines lattice (FLL).[12] In fact, the study of the magnetic-field (H) temperature (T) phase diagram of iron-based superconductors has immediately attracted a lot of interest owing to their extremely high upper critical fields,[13,14] which in some cases reach values even larger than those of high-T_c superconductors.

Most of the theories aiming at describing the FLL properties are based on a regular arrangement of vortices.[15] However, in real crystals this is far from being the case, because crystal defects, such as dislocations or inclusions, usually act as pinning centers preventing the vortices from having a regular arrangement or from moving freely under the action of an electric current. Since these dynamics lead to dissipative effects the study of the pinning potential is of major importance for the technological applications of superconductors. On the other hand, the understanding of the different phases developing in the magnetic-field temperature phase diagram of a superconductor and the modeling of the different dynamical regimes give rise to fundamental questions.[16] A technique which offers the possibility of studying the FLL dynamics from a microscopic point of view is nuclear magnetic resonance (NMR). In the past years a fruitful study was performed in the cuprates[17–19] and showed that the linewidth and the spin-lattice relaxation times were effective markers of the vortex dynamics. Moreover, these two quantities provide complementary information since the linewidth narrowing is sensitive to the magnetic-field fluctuations along the direction of the external field, while the spin-lattice relaxation time is sensitive to the transverse fluctuations. Furthermore, being the nuclei local probes they are sensitive to flux lines excitations at all wave vectors,[20] at variance with macroscopic techniques, as the ac susceptibility, for example, which are sensitive just to the long-wavelength excitations.[21]

Thanks to the works performed in the cuprates we know now that in very anisotropic superconductors vortices can be considered as independent two-dimensional isles called "pancakes" which undergo diffusive thermal motions.[22,23] Bearing this in mind, and looking at the structural similarities between cuprates and pnictides, some obvious questions arise: is it still possible to detect the vortices thermal dynamics in iron pnictides with NMR? What is the vortices structure in the new iron-based compounds? Are vortices two-dimensional (2D) uncorrelated islands or rather three-dimensional structures? In order to answer at least part of these open questions we performed an NMR study of the superconducting state of $Ba(Fe_{1-x}Rh_x)_2As_2$ superconductor with $x \sim 0.07$. We measured both the spin-lattice ($1/T_1$) and spin-echo ($1/T_2$) relaxation rates of the ^{75}As nuclei, together with the Knight shift and the NMR linewidth, at two different field intensities (7 and 3 T) and orientations ($\mathbf{H} \parallel$ or $\perp c$). The study of these quantities evidences the presence of low-frequency dynamics that we interpreted in the light of FLL motion and, accordingly, we derived a quantitative description of the vortex motions, namely the temperature dependence of the correlation time and of the pinning potential at different magnetic fields. In the present work we will concentrate solely on the superconducting properties, while the discussion of the normal state will be presented in a future study.

II. TECHNICAL ASPECTS AND EXPERIMENTAL RESULTS

^{75}As NMR measurements were performed on a flat $0.8 \times 5 \times 7$ mm^3 parallelepiped-shaped crystal of $Ba(Fe_{0.93}Rh_{0.07})_2As_2$ with the c axis along the shortest side. The sample was grown by the self-flux method according to a procedure reported in Ref. 13. The phase diagram of Rh-doped compounds shows many similarities with that of Co-doped compounds and the maximum estimated transition

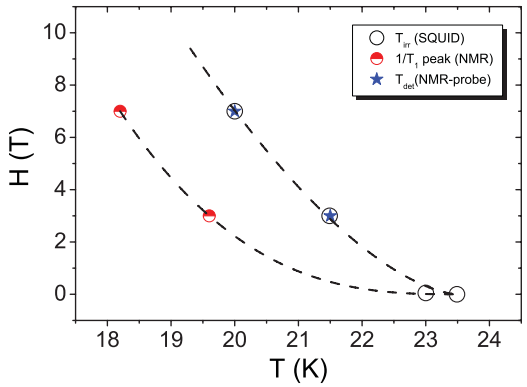

FIG. 1. (Color online) The irreversibility temperature measured with a dc SQUID magnetometer (open circle) is compared with that derived from the detuning of the NMR probe (blue stars). The red circles refer to the temperature of the peaks in $1/T_1$. The dotted lines are a guide to the eye.

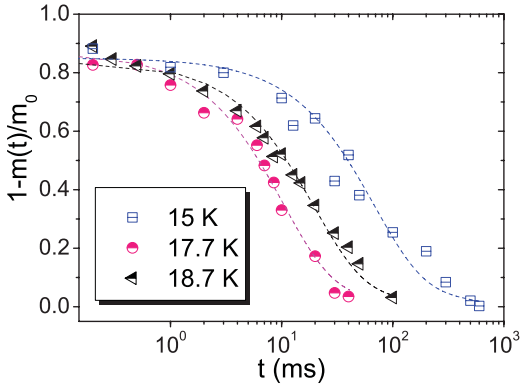

FIG. 2. (Color online) The recovery curves for three different temperatures are shown, for $\mathbf{H} \parallel c$, at 7 T. The blue squares refers to the 15-K data, while the pink circles are taken at 17.7 K, in correspondence with the peak in $1/T_1$, and the black triangles refer to 18.7 K. The dotted colored lines are the best fits according to Eq. (1).

temperature is about 23 K (Ref. 14) for the optimally doped $x \simeq 0.07$ system. For such Rh concentration both the structural and antiferromagnetic phase transitions are suppressed. To provide a first characterization of the crystal we measured the field-cooled (FC) and zero-field-cooled (ZFC) magnetization by means of a Quantum Design MPMS-XL7 superconducting quantum interference device (SQUID) magnetometer. The irreversibility line was estimated looking at the temperature where the ZFC curve departs from the FC one, as in Ref. 24. This is the temperature where the magnetization is sensitive to a change in the dynamics of the FLL. On the other hand the detuning of the NMR probe[17] is a higher frequency measurement which, nevertheless, is found to be consistent with what is observed in static field measurements (Fig. 1).

The NMR measurements were performed by using standard radio frequency pulse sequences. The spin-lattice relaxation time T_1 was measured by means of a saturating recovery pulse sequence at two different magnetic fields $H = 7$ T and 3 T. The recovery of the nuclear magnetization $m(t)$ was found to follow the relation[25,26]

$$1 - m(t)/m_0 = 0.1e^{-t/T_1} + 0.9e^{-6t/T_1} \qquad (1)$$

expected for a nuclear spin $I = 3/2$ in the case of a magnetic relaxation mechanism (see Fig. 2). In the normal phase $1/T_1T$ shows a temperature-independent behavior, as expected for a weakly correlated metal (see the inset to Fig. 3).[27] By decreasing the temperature below T_c we observed a well-defined peak in $1/T_1$ for $\mathbf{H} \parallel c$. The peak temperature decreased by increasing the magnetic-field intensity (see Fig. 3). Remarkably when $\mathbf{H} \perp c$ the peak in $1/T_1$ disappears (see Fig. 4). At lower temperatures $1/T_1$ decreases exponentially and it is only weakly dependent on the magnetic-field orientation.

The transverse relaxation time T_2 was measured by recording the decay of the echo after a $\pi/2 - \tau - \pi$ pulse sequence as a function of the delay τ. Since the functional form of the decay changes with temperature (Fig. 5), as will be discussed subsequently, in order to compare the data over the full temperature range we defined T_2 as the time where the echo amplitude decreases by $1/e$.

In the normal phase $1/T_2$ shows an activated temperature dependence whose origin will be discussed elsewhere. Below T_c we observed a marked increase in $1/T_2$ giving rise to a peak around 12–13 K, for $\mathbf{H} \parallel c$. We note that Oh *et al.* found a similar behavior in a 7.4% Co-doped single crystal, with a peak around 15 K.[28] Nevertheless, we note that in their sample the amplitude of the peak in $1/T_2$ is lower for magnetic fields close to the ones used here and only for $H = 16.8$ T they recover an amplitude of the peak similar to the one found in our system. This indicates that for magnetic fields around 7 T the root-mean-square amplitude of the fluctuating field is larger for our 7% Rh-doped compound rather than for the 7.4% Co-doped one. This suggests a higher mobility in the former system. By further decreasing the temperature, for $T \to 0$ the spin-echo decay rate is found to reach the value derived by Van Vleck lattice sums, as it has to be expected for a frozen vortex lattice, where the spin dephasing is provided by nuclear dipole-dipole interaction.

Similarly to what was observed for $1/T_1$, also the $1/T_2$ peak gets significantly reduced for $\mathbf{H} \perp c$ (Fig. 6).

The NMR spectrum was determined from the Fourier transform of half of the ^{75}As echo signal, while below $T \simeq$

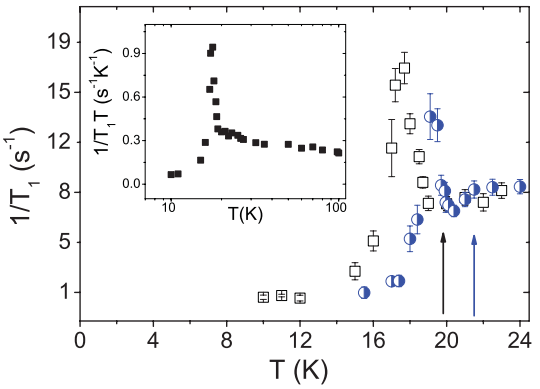

FIG. 3. (Color online) The spin-lattice relaxation rate, measured at 7 T (open squares) and 3 T (blue circles), for $\mathbf{H} \parallel c$ is reported. The inset shows the $1/T_1T$ data at 7 T both in the superconducting and normal phase. The arrows show the temperature of the detuning of the NMR probe at the two fields: the blue arrow stands for 3 T and the black arrow for 7 T.

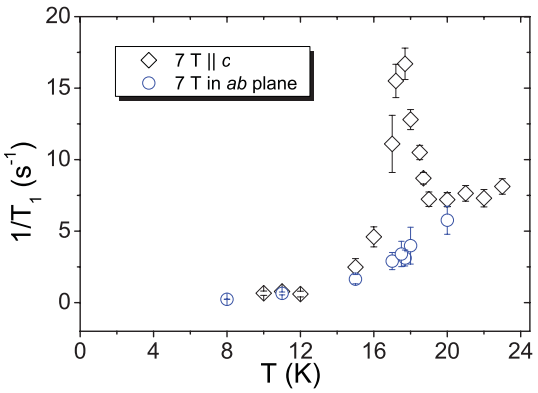

FIG. 4. (Color online) The spin-lattice relaxation rate, measured at 7 T, in $\mathbf{H} \parallel c$ geometry (black diamonds) and $\mathbf{H} \perp c$ geometry (blue circles) is shown. A neat difference for the two field orientations is found in the 16–19-K range. Data, in $\mathbf{H} \perp c$ geometry, have been normalized by a value 1.55 to match the value of $1/T_1$ for $\mathbf{H} \parallel c$, at T_c thus revealing an anisotropy of the hyperfine tensor.

13 K, when the line became too broad, the spectrum was derived by sweeping the irradiation frequency. The full width at half maximum (FWHM) was determined by a Gaussian fit. In the normal state the linewidth increased on cooling following a Curie-Weiss trend (Fig. 7), probably due to the presence of paramagnetic impurities. The impurities cause the appearance of a staggered magnetization and a broadening of the NMR line. On the other hand, the average magnetic field is only weakly affected, so we do not expect an extra contribution to the shift.[29] After subtracting this impurity-dependent contribution $\Delta\nu_{NP}$ from the raw data by using the relation

$$\Delta\nu(T) \simeq \sqrt{\Delta\nu(T)^2_{\rm raw} - \Delta\nu^2_{NP}} \tag{2}$$

we observed that below T_c an extra broadening induced by the presence of the flux lines lattice appears (Fig. 7). The impurity-dependent contribution was found to be well described by the

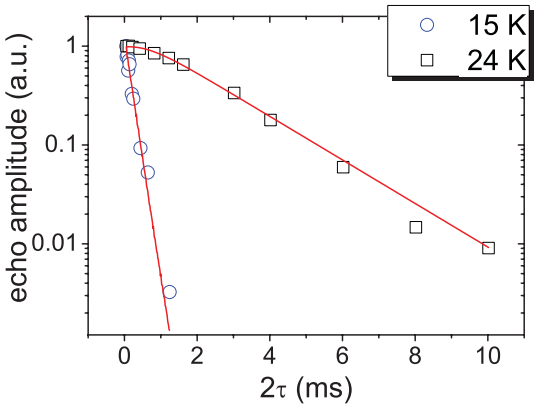

FIG. 5. (Color online) The figure shows two echo decays as a function of 2τ: the black squares refer to 24 K and the blue circles refer to 15 K, below the superconducting transition where the FLL is still dynamic. From the figure one can notice that the echo decay functional form changes while the temperature decreases. The red curves are the best fits according to Eqs. (10) and (11).

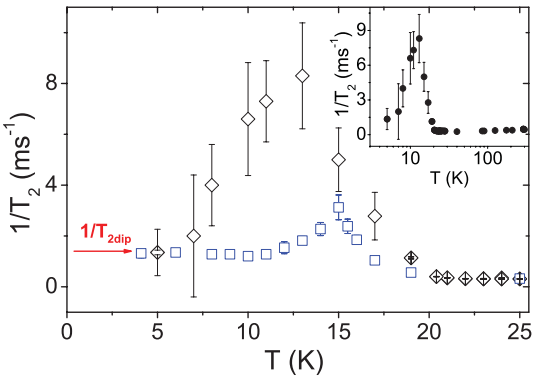

FIG. 6. (Color online) The figure shows the spin-echo decay rate measured at 7 T. A peak around 12 K is found for $\mathbf{H} \parallel c$ (black diamonds) while it strongly decreases, for $\mathbf{H} \perp c$ (blue squares), and shifts toward higher temperatures. The red arrow indicates the *ab initio* value for $1/T_2$ given by the dipolar sums. The inset shows the spin-echo decay rate for $\mathbf{H} \parallel c$ up to room temperature.

Curie-Weiss relation, for both the sample orientations:

$$\Delta\nu_{NP}(T) = \frac{C}{T-\theta} + A. \tag{3}$$

By assuming the value of $\theta = -60$ K, as found by the fitting procedure we obtained the following results: for the $\mathbf{H} \parallel c$ case the fit gave $C = 1319 \pm 118$ kHz K and $A = 20.8 \pm 1$ kHz, while for the perpendicular geometry the fit gave $C = 1264 \pm 50$ kHz K and $A = 23.4 \pm 0.1$ kHz.

It has to be noticed that the superconducting state affects not only the ^{75}As NMR linewidth but also the NMR shift. Above T_c, in the normal phase, the NMR shift shows an activated behavior, as observed also for the Co-doped $BaFe_2As_2$.[28] The experimental data (Fig. 8) can be fit with an activated Arrhenius law: $y = A + B\exp(-D/T)$, yielding $A = 0.26\%$, $B = 0.071\%$, and $D = 225 \pm 22$ K, for $\mathbf{H} \parallel c$, in good agreement with the values found in Ref. 28. Below T_c the shift starts to decrease as expected for a singlet state pairing.[30] In the superconducting phase the NMR shift $K(T)$ can be assumed to result from three contributions:

$$K(T) = K_{\rm spin}(T) + K_{FL}(T) + K_{TI}, \tag{4}$$

where $K_{\rm spin}(T)$ is the spin-dependent part, which vanishes for $T \to 0$, $K_{FL}(T)$ is the diamagnetic correction due to the vortex lattice, and the last term contains all the temperature-independent contributions (chemical shift, orbital terms, etc.).[31] Owing to the line broadening and to the reduction in the radio frequency penetration depth, the accuracy in the estimate of $K(T)$ decreases below T_c and does not allow us to draw convincing conclusions on the symmetry of the order parameter.

Taking into account the quadrupolar shift of the central line, in the transverse geometry, we estimated a quadrupolar frequency $\nu_Q(100\ {\rm K}) \sim 1.5$ MHz, very close to the one found in the parent compound.[25]

III. DISCUSSION

As previously mentioned, here we will not discuss the normal state properties but rather we shall concentrate on the

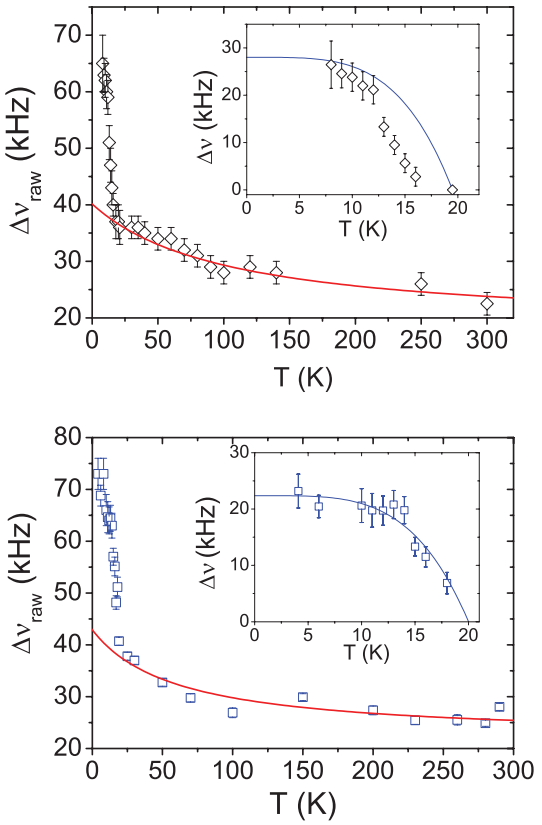

FIG. 7. (Color online) The two figures show the full width at half maximum of the central line at 7 T, for $\mathbf{H} \parallel c$ (top) and $\mathbf{H} \perp c$ (bottom), with the Curie-Weiss fit (red solid line) giving the impurity contribution [see Eq. (3) in the text]. In the insets the extra broadening due to the FLL, obtained as described by Eq. (2), is shown. The blue solid lines show the behavior expected according to a two-fluid model. For $\mathbf{H} \parallel c$ one can observe a strong deviation at high temperatures which is not seen for the other orientation. We notice that, at variance with what was reported by Oh *et al.* (Ref. 28) in the 7.4% Co-doped compound, here we do not observe any decrease in the linewidth below T_c.

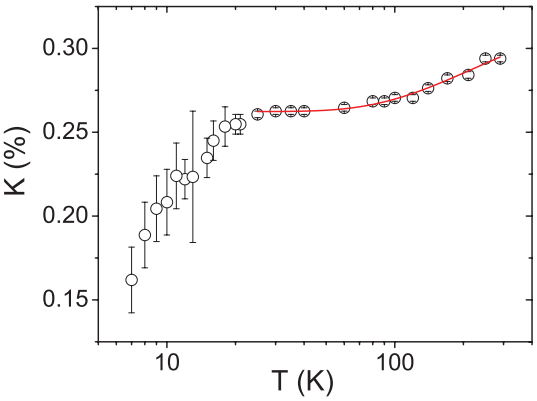

FIG. 8. (Color online) The figure shows the Knight shift at 7 T, for $\mathbf{H} \parallel c$ with an Arrhenius-like fitting curve (solid line) in the normal phase.

superconducting phase. Let us first consider the behavior of the spin-lattice relaxation rate which is characterized by a well defined peak for $\mathbf{H} \parallel c$ below T_c. In passing, we note that in Co optimally doped compound,[32] no peak was observed in $1/T_1$, below T_c. On the other hand Laplace *et al.*,[8] in a 6% Co-doped $BaFe_2As_2$, found a peak in $1/T_1$ just below T_c and an enhancement in $1/T_1T$ at higher temperature due to spin-density-wave correlations. The peak we found below T_c is not expected to be a Hebel-Slichter peak[33] since the majority of the experimental and theoretical results point toward an extended $s^{\pm}$-wave pairing,[2,4–6,34] where that feature is expected to be absent. Furthermore if it was a coherence peak the data would be described, below T_c, by $1/T_1 \sim e^{-\Delta/T}$ with Δ the superconducting gap. By fitting the data one obtains $\Delta \simeq 200$ K $\gg$ 3.5 $k_B T_c$, the value expected for the superconducting order parameter.[35] Finally, the striking suppression of the peak for $\mathbf{H} \perp c$ can hardly be reconciled with the small anisotropy of the electron spin susceptibility found in those materials. Hence that maximum in $1/T_1$ just below T_c should not be associated with the electron spin dynamics but, given the similarities with the behavior found in $HgBa_2CuO_{4+\delta}$ (Ref. 36) and $YBa_2Cu_4O_8$ (Ref. 37) cuprates, it is tempting to associate the $1/T_1$ peak to the FLL dynamics.

In order to analyze the experimental results one can start from the basic modeling of FLL in strongly anisotropic superconductors:[38] the vortices enter the sample in the form of quasi-two-dimensional pancakes, lying in the FeAs planes. Owing to the thermal excitations they move out of their equilibrium positions by means of random motions, which can be hindered by the pinning centers. Differently from cuprates, which exhibit a very high anisotropic ratio $\gamma = \xi_{ab}/\xi_c$, with ξ_{ab} and ξ_c the in-plane and out-of-plane coherence lengths, the Ba122 superconductors show $\gamma \sim 2$–4 varying with temperature.[14] This suggests to describe the flux lines not as completely uncorrelated pancakes, but rather as a stack of correlated islands. Still, since the estimated coherence length ξ_c is of the order of the interlayer distance s,[39] namely $2\xi_c \simeq s \simeq 6$ Å , FeAs planes can be considered as weakly coupled superconducting layers. Accordingly, when $\mathbf{H} \perp c$ the flux lines are preferentially trapped between the planes and the FeAs plane boundaries act as pinning centers, a well-known effect in layered superconductors. These intrinsic pinning centers hinder the dynamics and yield the observed suppression in the $1/T_1$ peak for $\mathbf{H} \perp c$.

In order to understand the shift of the $1/T_1$ peak upon increasing H we first recall that $1/T_1$ probes the spectral density $J(\omega_L)$ at the nuclear Larmor frequency ω_L, namely

$$\frac{1}{T_1} = \frac{\gamma^2}{2} \int \langle h_\rho(t) h_\rho(0) \rangle e^{-i\omega_L t} dt \qquad (5)$$

with h_ρ the magnetic-field component perpendicular to $\mathbf{H}$ and $\gamma = 2\pi \times 7.292 \times 10^6$ rad/T the gyromagnetic ratio of the ^{75}As nucleus. Then the field dependence of the peak in $1/T_1$ can be qualitatively understood by considering that at the peak temperature the characteristic frequency for FLL motions is close to ω_L. When the magnetic field increases, T_c decreases and so does $T_{\rm irr}$, hence the FLL dynamics remain fast over a broader temperature range and the maximum in $1/T_1$ is observed at lower temperature (Fig. 1). It is noticed that the peak in the spin-lattice relaxation rate appears just below the irreversibility temperature, in contrast with what was found

in the cuprates, where it is well below the irreversibility line, suggesting a higher FLL mobility in these latter compounds.[37]

To give a quantitative description of the peak we started from Eq. (5). Let us first assume that the vortex fluctuations are basically two dimensional (2D), that they take place in a spatial range smaller than the intervortex distance[40] $l_e = \sqrt{2/\sqrt{3}}\sqrt{\Phi_0/H}$ (for a triangular FLL), and that they move by Brownian motions[36,37] described by a diffusive-like correlation function $g_1(t) = \exp(-D_\perp q_\perp^2 t)$, $D_\perp$ being the diffusion constant of the motion taking place in the ab plane. Then $\tau_c(q_\perp) = 1/D_\perp q_\perp^2$ plays the role of a q-dependent correlation time for the collective vortex motions. By summing over all collective in-plane excitations up to a cutoff wave vector $q_m = (1/l_e)(8\pi^3/3)^{1/4}$ Suh *et al.*[36] found the spectral density

$$J(\omega_L) = \tau_m \ln\left[\frac{\tau_m^{-2} + \omega_L^2}{\omega_L^2}\right], \tag{6}$$

where the average correlation time is $\tau_m = 1/D_\perp q_m^2$. For the temperature dependence of τ_m it is reasonable to assume an activated form $\tau_m(T) = \tau_0 \exp(U/T)$, where U is an average pinning energy barrier and τ_0 stands for the correlation time in the infinite temperature limit. Accordingly an activated temperature dependence of the spectral density at the Larmor frequency and then of $1/T_1$ are observed for $T \to 0$. The best fits of the data according to this 2D vortex model are reported in Fig. 9. It is noticed that the fit is not fully satisfactory.

On the other hand, as previously pointed out, the low anisotropy of $BaFe_2As_2$ compounds suggests that significant vortex correlations along the c axes are present in $Ba(Fe_{0.93}Rh_{0.07})_2As_2$. Thus the flux lines have to be considered as stationary waves oscillating in between the pinning centers. In order to take into account this effect we introduced empirically a modulation in the amplitude of the correlation function characterized by a wavelength λ which has an upper bound given by λ_c, the London penetration depth along the c axes. Then one can write $g_2(t) = \exp(-D_\perp q_\perp^2 t)\cos(z/\lambda)$. Now if we recall the form of the longitudinal field correlation function,[37]

$$\langle h_\rho(0)h_\rho(t)\rangle = \frac{\Phi_0^2 s^2}{4\pi\lambda_c^4}\langle u^2\rangle \frac{1}{\xi^2}\frac{1}{l_e^2\sqrt{3}} g_2(t), \tag{7}$$

and taking the root-mean-square amplitude of the vortex core fluctuation with respect to equilibrium position,[41,42]

$$\langle u^2\rangle \simeq \frac{\sqrt{2\pi\sqrt{3}}}{\Phi_0^2}\lambda_c\lambda_{ab} l_e k_B T,$$

Eq. (7) can be written as

$$\langle h_\rho(0)h_\rho(t)\rangle = \sqrt{\frac{3}{8\pi}}\frac{s^2 k_B T}{l_e}\frac{\lambda_{ab}(T)}{\lambda_c^3(T)\xi^2(T)} g_2(t), \tag{8}$$

where the temperature dependence is evident. Taking the values for the London penetration depth reported in the literature,[43] the coherence lengths derived from the H_{c2} measurements, and their temperature dependence according to the two-fluid model, we were able to reproduce fairly well the temperature dependence of $1/T_1$, which indicates that indeed a "3D-correlated-vortices" model is more appropriate

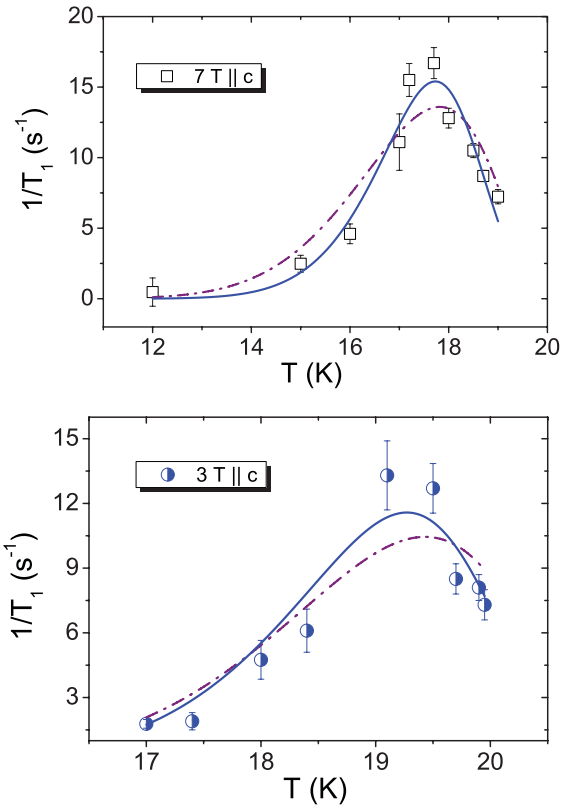

FIG. 9. (Color online) The figure at the top shows the spin-lattice relaxation rate at 7 T for $\mathbf{H} \parallel c$, while the one at the bottom shows the spin-lattice relaxation rate at 3 T in the same geometry. The fitting curves are given by the 2D uncorrelated pancakes model, deriving from the correlation function $g_1(t)$ (dash-dotted line) and the correlated vortices model, deriving from the correlation function $g_2(t)$ (solid line). In both cases the second model shows the best agreement with the experimental data.

to describe $Ba(Fe_{1-x}Rh_x)_2As_2$ superconductors. The best fits of the experimental results (Fig. 9) gives a value of $U = 322 \pm 66$ K for $H = 7$ T and $U = 470 \pm 5$ K for $H = 3$ T. These values are similar in magnitude to those found in YBCO-124,[37] nonetheless the quality of the fitting procedure suggests that the vortices develop a three-dimensional correlation. Before concluding this part we estimate the root-mean-square amplitude of the transverse field fluctuations $\langle h_e^2\rangle$ which represents the ripple of the magnetic-field profile modulated by the flux lines dynamics. In fact, given Eqs. (5) and (8), $1/T_1$ can be written in this new form, $1/T_1 = (\gamma^2/2)\langle h_e\rangle^2 J(\omega_L)$, from which we obtained $h_e \sim 30$–40 G at 7 T and ~ 20 G at 3 T. We point out that these values are close to the low-temperature NMR full width at half maximum, as it has to be expected.

While the spin-lattice relaxation rate has been considered one of the most valuable microscopic probes of the FLL motion, not so much effort has been devoted to the analysis of the spin-echo decay time, mainly because its interpretation is not always straightforward.[44,45] As it has been already pointed out in the superconducting state $1/T_2$ shows a neat anisotropy: the peak found for $\mathbf{H} \parallel c$ is significantly reduced and shifted in the $\mathbf{H} \perp c$ configuration. Moreover, we point out that at low temperature $1/T_2$ reaches the value expected from the Van Vleck lattice sums.[28,46] In fact, at low temperatures all

dynamics are frozen and the only process giving rise to the echo decay is the nuclear dipole-dipole interaction. The peak observed around 10 K cannot be due to a time-dependent modulation of that interaction since we do not expect such an anisotropic behavior, in that case. On the other hand, given the similarity with $1/T_1$ peak anisotropy, it is likely that also a $1/T_2$ peak arises from a low-frequency vortex dynamics. Nevertheless, it should be emphasized that while $1/T_1$ measurements are sensitive to the fluctuations of the transverse components of the magnetic field, $1/T_2$ is sensitive to the longitudinal ones. In particular, it should be noticed that when the vortices are strongly correlated along the c axes, the flux lines move rigidly and do not affect significantly the transverse field components, while they do change the longitudinal ones.[42] Hence the information derived from those two types of measurements can be complementary.

In order to analyze the temperature dependence of $1/T_2$ we need an analytical expression for the spin-echo decay. In principle we should start from a relation similar to Eq. (7), nevertheless here, for the sake of simplicity, we assumed an exponential correlation function for the longitudinal field fluctuations,

$$\langle h_l(0)h_l(t)\rangle = \langle h_l^2\rangle e^{-t/\tau_L}, \tag{9}$$

characterized by an average correlation time τ_L. Correspondingly we have written the decay of the echo amplitude as a function of the delay τ between the $\pi/2$ and π pulses in the echo sequence as[47]

$$M(2\tau) = M_0 e^{-2\tau/T_{2dip}^2} \times M_2(2\tau), \tag{10}$$

$$M_2(2\tau) = e^{-\gamma^2\langle h_l^2\rangle\tau_L^2[2\tau/\tau_L+4\exp(-2\tau/\tau_L)-\exp(-2\tau/\tau_L)-3]}, \tag{11}$$

where the first Gaussian term accounts for the nuclear dipole-dipole contribution, while the second term describes the low-frequency vortex motions. By fitting the data below T_c we were able to derive the temperature dependence of the longitudinal correlation time (Fig. 10). By decreasing the temperature the FLL motion is supposed to go through different motional regimes: from the fast motions ($\tau_L \ll T_2$) up to the very slow motions ($\tau_L \gg T_2$), where the correlation time is so long that

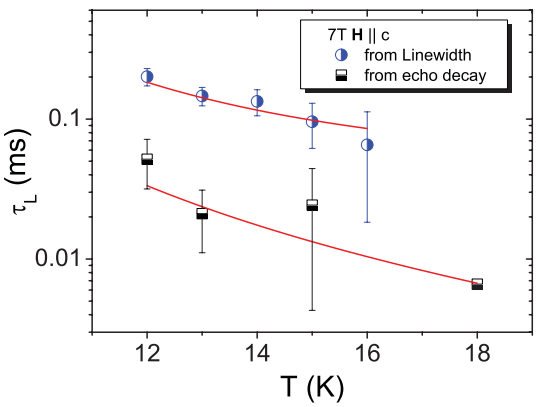

FIG. 10. (Color online) The temperature dependence of the correlation time τ_L given by echo decay time (black squares) is compared with the one derived by the linewidth analysis (blue circles) in the assumption of fast motions [see Eq. (12)]. The red curves are the fitting of the correlation time, according to an activated law.

we can consider the FLL to be frozen in the solid state. If we fit the data above 11 K, where the peak in $1/T_1$ is observed, we notice that τ_L follows an activated behavior characterized by an activation barrier $U_L \simeq 50$ K much lower than the one derived from $1/T_1$ (see Fig. 10). Here we refer just to the fast motion limit, since the fitting procedure is not so much accurate at the low temperatures, because of the reduced signal-to-noise ratio.

The correlation time derived from the spin-echo decay rate can be suitably compared to that derived from the motional narrowing of the NMR line. The latter can be derived, for the $\mathbf{H} \parallel c$ case, following the standard approach reported in Ref. 48. In the fast motions regime, namely $2\pi\overline{(\Delta\nu_R)^2}^{1/2}\tau_L \ll 1$, with $\overline{(\Delta\nu_R)^2}^{1/2}$, the square root of the rigid lattice second moment, one has

$$\Delta\nu \simeq \tau_L \frac{\overline{(\Delta\nu_R)^2}}{2\pi}. \tag{12}$$

By fitting the correlation time τ_L with an Arrhenius's law we extracted a pinning energy barrier $U_L = 48 \pm 3$ K, which is consistent with the one derived from the spin-echo decay measurements. This is not surprising since both T_2 and $\Delta\nu$ probe the longitudinal component of the local-field fluctuation.

In order to understand why the energy barrier probed by $1/T_2$ and from the motional narrowing are smaller than the one derived from $1/T_1$ measurements it should be pointed out that the oscillations at wave vector $q_\parallel \to 0$ do contribute to the longitudinal field fluctuations but only weakly to the transverse field excitations which are relevant in $1/T_1$, at variance with the $q_\parallel \to 1/s$ modes, which contribute significantly to $1/T_1$. Hence, our findings indicate that the energy cost to activate a certain collective mode increases with increasing $q_\parallel$, where the $\parallel$ subscript refers to the wave-vector component parallel to the magnetic field.

Upon cooling the crystal to the lowest temperatures we observed a change in the line shape from Lorentzian to Gaussian, as has to be expected when the correlation time gets longer than a few ms. The Gaussian line shape, instead of the asymmetric one expected for a perfect triangular lattice, indicates the presence of lattice distortions induced by randomly distributed pinning centers. In this scenario one can only make an estimate of the London penetration depth which can be compared with the one derived by transverse μSR,[49] transport,[43] and the tunnel diode resonator measurements[50] on a similar 7.4% Co-doped $BaFe_2As_2$ single crystal. These authors report λ_{ab} values between 200 and 217 nm. Following Ref. 51 we extracted

$$\lambda_{ab} = \sqrt{\frac{2.36\Phi_0\gamma\sqrt{k}}{\Delta\nu}}, \tag{13}$$

where $\sqrt{k} = 0.043\,24$ depends on the lattice geometry and on the magnitude of the applied field. Taking $\Delta\nu(T \to 0) \simeq 30$ kHz, for $\mathbf{H} \parallel c$ we extracted $\lambda_{ab}(0) \sim 226 \pm 9$ nm, in agreement with the former results.

IV. CONCLUSIONS

This work aimed at studying the thermally activated vortices motion, by means of ^{75}As microscopic probe. We found that in the NMR relaxation rates and in the NMR linewidth there

is evidence of such motions, which is well supported by the remarkably anisotropic behavior of those quantities. We were able to follow the dynamics of the vortices by measuring NMR quantities which are sensitive to motions at different time scales: the peak in the spin-lattice relaxation time is found when the correlation time is about 10^{-7}–10^{-8} s, while the $1/T_2$ maximum occurs at a slightly lower temperature, when the correlation time is comparable to $1/T_2$, i.e., few ms. In the temperature window between those peaks the motions are effective and yield the motional narrowing of the NMR line. To observe a line narrowing the correlation times must be smaller than the inverse of the rigid lattice linewidth $\sim 10^{-4}$ s. Furthermore, we pointed out that the temperature dependence of $1/T_1$ around the peak suggests that the flux lines are formed by strongly coupled vortices rather than nearly independent pancakes diffusing in two dimensions, as it was found in the cuprates.

ACKNOWLEDGMENTS

We gratefully acknowledge A. Rigamonti for useful discussions, and M. Moscardini for his help in setting up the experiments.

[1] Y. Kamihara, T. Watanabe, M. Hirano, and H. Hosono, J. Am. Chem. Soc. **130**, 3296 (2008).
[2] H. Ding, P. Richard, K. Nakayama, T. Arakane, Y. Sekiba, A. Takayama, S. Souma, T. Sato, T. Takahashi, Z. Wang, X. Dai, Z. Fang, G. F. Chen, J. L. Luo, and N. L. Wang, Europhys. Lett. **83**, 47001 (2008).
[3] T. Kondo, A. F. Santander-Syro, O. Copie, C. Liu, M. E. Tillman, E. D. Mun, J. Schmalian, S. L. Bud'ko, M. A. Tanatar, P. C. Canfield, and A. Kaminski, Phys. Rev. Lett. **101**, 147003 (2008).
[4] P. Szabo, Z. Pribulova, G. Pristas, S. L. Budko, P. C. Canfield, and P. Samuely, Phys. Rev. B **79**, 012503 (2009).
[5] G. Mu, H. Luo, Z. Wang, L. Shan, C. Ren, and H. H. Wen, Phys. Rev. B **79**, 174501 (2009).
[6] K. Terashima, Y. Sekiba, J. H. Bowen, K. Nakayama, T. Kawahara, T. Sato, P. Richard, Y.-M. Xu, L. J. Li, G. H. Cao, Z.-A. Xu, H. Ding, and T. Takahashi, Proc. Natl. Acad. Sci. USA **106**, 7330 (2009).
[7] S. Sanna, R. De Renzi, T. Shiroka, G. Lamura, G. Prando, P. Carretta, M. Putti, A. Martinelli, M. R. Cimberle, M. Tropeano, and A. Palenzona, Phys. Rev. B **82**, 060508(R) (2010).
[8] Y. Laplace, J. Bobroff, F. Rullier-Albenque, D. Colson, and A. Forget, Phys. Rev. B **80**, 140501(R) (2009).
[9] C. Fang, Y. Wu, R. Thomale, B. Andrei Bernevig, and J. Hu, Phys. Rev. X**1**, 011009 (2011).
[10] I. I. Mazin, D. J. Singh, M. D. Johannes, and M. H. Du, Phys. Rev. Lett. **101**, 057003 (2008).
[11] I. I. Mazin, M. D. Johannes, L. Boeri, K. Koepernik, and D. J. Singh, Phys. Rev. B **78**, 085104 (2008).
[12] G. Blatter, M. Y. Feigel'man, Y. B. Geshkenbein, A. I. Larkin, and V. M. Vinokur, Rev. Mod. Phys. **66**, 1125 (1994).
[13] N. Ni, A. Thaler, A. Kracher, J. Q. Yan, S. L. Bud'ko, and P. C. Canfield, Phys. Rev. B **80**, 024511 (2009).
[14] N. Ni, M. E. Tillman, J.-Q. Yan, A. Kracher, S. T. Hannahs, S. L. Bud'ko, and P. C. Canfield, Phys. Rev. B **78**, 214515 (2008).
[15] A. A. Abrikosov, Sov. Phys. JETP **5**, 1174 (1957).
[16] P. Gammel, Nature (London) **411**, 434 (2001).
[17] P. Carretta, Phys. Rev. B **45**, 5760(R) (1992).
[18] A. Rigamonti, F. Borsa, and P. Carretta, Rep. Prog. Phys. **61**, 1367 (1998).
[19] P. Carretta, Phys. Rev. B **48**, 528 (1993).
[20] D. A. Torchetti, M. Fu, D. C. Christensen, K. J. Nelson, T. Imai, H. C. Lei, and C. Petrovic, Phys. Rev. B **83**, 104508 (2011).
[21] G. Prando, P. Carretta, R. De Renzi, S. Sanna, A. Palenzona, M. Putti, and M. Tropeano, Phys. Rev. B **83**, 174514 (2011).
[22] P. W. Anderson and Y. B. Kim, Rev. Mod. Phys. **36**, 39 (1964).
[23] M. Tinkham, *Introduction to Superconductivity*, 2nd ed. (Dover, New York, 1996).
[24] A. Lascialfari, A. Rigamonti, E. Bernardi, M. Corti, A. Gauzzi, and J. C. Villegier, Phys. Rev. B **80**, 104505 (2009).
[25] H. Fukazawa, K. Hirayama, K. Kondo, T. Yamazaki, Y. Kohori, N. Takeshita, K. Miyazawa, H. Kito, H. Eisaki, and A. Iyo, J. Phys. Soc. Jpn. **77**, 105004 (2008).
[26] W. W. Simmons, W. J. O'Sullivan, and W. A. Robinson, Phys. Rev. **127**, 1168 (1962).
[27] C. P. Slichter, *Principles of Magnetic Resonance*, Springer Series In Solid-State Sciences No. 1, 3rd enlarged and updated ed. (Springer, New York, 1996).
[28] S. Oh, A. M. Mounce, S. Mukhopadhyay, W. P. Halperin, A. B. Vorontsov, S. L. Bud'ko, P. C. Canfield, Y. Furukawa, A. P. Reyes, and P. L. Kuhns, Phys. Rev. B **83**, 214501 (2011).
[29] H. Alloul, J. Bobroff, M. Gabay and P. J. Hirschfeld, Rev. Mod. Phys. **81**, 45 (2009).
[30] K. Yosida, Phys. Rev. **110**, 769 (1958).
[31] D. E. MacLaughlin, *Solid State Physics: Advances in Research and Applications*, Vol. 3 (Academic, London, 1976).
[32] F. Ning, K. Ahailan, T. Imai, A. S. Sefat, R. Jin, M. A. McGuire, B. C. Sales, and D. Mandrus, J. Phys. Soc. Jpn. **77**, 103705 (2008).
[33] L. C. Hebel and C. P. Slichter, Phys. Rev. **113**, 1504 (1959).
[34] D. Parker, O. V. Dolgov, M. M. Korshunov, A. A. Golubov, and I. I. Mazin, Phys. Rev. B **78**, 134524 (2008).
[35] K. Nakayama, T. Sato, P. Richard, Y.-M. Xu, Y. Sekiba1, S. Souma, G. F. Chen, J. L. Luo, N. L. Wang, H. Ding, and T. Takahashi, Eur. Phys. Lett. **85**, 67002 (2009).
[36] B. J. Suh, F. Borsa, J. Sok, D. R. Torgeson, M. Corti, A. Rigamonti, and Q. Xiong, Phys. Rev. Lett. **76**, 1928 (1996).
[37] M. Corti, B. J. Suh, F. Tabak, A. Rigamonti, F. Borsa, M. Xu, and B. Dabrowski, Phys. Rev. B **54**, 9469 (1996).
[38] E. H. Brandt, Physica B **169**, 91 (1991).
[39] M. Rotter, M. Tegel, D. Johrendt, I. Schellenberg, W. Hermes, and R. Pottgen, Phys. Rev. B **78**, 020503(R) (2008).
[40] M. Cyrot and D. Pavuna, *Introduction to Superconductivity and High-Tc Materials* (World Scientific, Singapore, 1995).
[41] H. E. Brandt, Physica C **195**, 1 (1992).
[42] J. R. Clem, Phys. Rev. B **43**, 7837 (1991).
[43] M. A. Tanatar, N. Ni, C. Martin, R. T. Gordon, H. Kim, V. G. Kogan, G. D. Samolyuk, S. L. Bud'ko, P. C. Canfield, and R. Prozorov, Phys. Rev. B **79**, 094507 (2009).

[44]B. J. Suh, D. R. Torgeson, and F. Borsa, Phys. Rev. Lett. **71**, 3011 (1993).
[45]C. H. Recchia, J. A. Martindale, C. H. Pennington, W. L. Hults, and J. L. Smith, Phys. Rev. Lett. **78**, 3543 (1997).
[46]S. Mukhopadhyay, S. Oh, A. M. Mounce, M. Lee, W. P. Halperin, N. Ni, S. L. Bud'ko, P. C. Canfield, A. P. Reyes, and P. L. Kuhns, New J. Phys. **11**, 055002 (2009).
[47]M. Takigawa and G. Saito, J. Phys. Soc. Jpn. **55**, 1233 (1986).
[48]A. Abragam, *The Principles of Nuclear Magnetism* (Oxford Univesity Press, New York, 1961).
[49]T. J. Williams, A. A. Aczel, E. Baggio-Saitovitch, S. L. Bud'ko, P. C. Canfield, J. P. Carlo, T. Goko, H. Kageyama, A. Kitada, J. Munevar, N. Ni, S. R. Saha, K. Kirschenbaum, J. Paglione, D. R. Sanchez-Candela, Y. J. Uemura, and G. M. Luke, Phys. Rev. B **82**, 094512 (2010).
[50]R. T. Gordon, N. Ni, C. Martin, M. A. Tanatar, M. D. Vannette, H. Kim, G. D. Samolyuk, J. Schmalian, S. Nandi, A. Kreyssig, A. I. Goldman, J. Q. Yan, S. L. Budko, P. C. Canfield, and R. Prozorov, Phys. Rev. Lett. **102**, 127004 (2009).
[51]E. H. Brandt, Phys. Rev. B **37**, 2349(R) (1988).